QUANTUM CHEMICAL STUDIES OF (E)-1-((PHENYLIMINO)METHYL)NAPHTHALEN-2-OL AND (E)-1-(((4-CHLOROPHENYL)IMINO)METHYL)NAPHTHALEN-2-OL

DEMEHIN, A. I.
Department of Chemistry, Adeyemi Federal University of Education, Ondo
demehinai@gmail.com

Abstract
(E)-1-((phenylimino)methyl)naphthalen-2-ol (L_1) and (E)-1-(((4-chlorophenyl)imino)methyl) naphthalen-2-ol (L_2) were synthesized and characterized by elemental analysis, infrared, ultraviolet-visible, proton and carbon-13 spectroscopies. Theoretical calculations were also performed on the modelled and optimized structures using Density Functional Theory (DFT) with Becke's three-parameter hybrid functional employing the Lee-Yang-Parr correlation functional (B3LYP) and the Empirical Density Functional 1 methods (EDF1) with 6-31G** basis set. The infrared, ultraviolet, proton and carbon-13 nuclear magnetic resonance spectra of the compounds were calculated and the results compared with the corresponding experimental spectra to boost the structural elucidation. The comparison between the calculated and experimental results provided a very good agreement.

Keywords: Quantum chemical study, (E)-1-((phenylimino)methyl)naphthalen-2-ol, (E)-1-(((4-chlorophenyl)imino)methyl) naphthalen-2-ol, Schiff base, substituent

Introduction

(E)-1-((phenylimino)methyl)naphthalen-2-ol and (E)-1-(((4-chlorophenyl)imino)methyl) naphthalen-2-ol are Schiff bases. A Schiff base is similar to an aldehyde or ketone, but for the carbonyl (C=O) group, which is replaced with an azomethine (HC=N) group. They were discovered by Hugo Schiff in 1864 (Belal et al., 2015; Bitu et al., 2019; Thangadurai et al., 2020) and have the general formula $RR_1C{=}N{-}R_2$. If R equals hydrogen, alkyl or aryl, R_1 hydrogen and R_2 alkyl or aryl; the compounds are referred to as aldimines ($R_1{-}CH{=}NR_2$) while compounds where both R and R_1 are alkyl or aryl groups are called ketimines. R_2 can either be an alkyl or an aryl group. Schiff bases can also be called azomethines or imines (Kubra et al., 2018; Omidi & Kakanejadifard, 2020). They are significant chelating ligands in coordination chemistry, and the chemical properties can be altered by varying the substituents on either the carbonyl or the amine ring. Intra- and intermolecular hydrogen bonds can be formed from Schiff bases obtained from naphthaldehyde and its different derivatives, which usually determine their chemical and physicochemical properties (Abo-Aly et al., 2015; Belal et al., 2015; Shajari & Yahyaei, 2020; Thangadurai et al., 2020).

Schiff bases have vital donor atoms like nitrogen and oxygen, which make them resemble living systems and display different biological properties. The resulting imines in Schiff bases are involved in binding with metal ions via nitrogen lone pair of electrons; these can bind to the central metal ions as monodentates and polydentates (Bitu et al., 2019; Kianfar et al., 2015). The imine groups are significant for the biological activities of Schiff bases and are very useful active centres of many biological systems (Kubra et al., 2018; Sayed et al., 2020). Schiff bases lead to the

formation of many mononuclear and binuclear complexes with different coordination modes and stereochemistry (Saranya et al., 2020; Zhang et al., 2018).

Schiff bases have played essential roles in understanding the coordination chemistry of transition metal ions. Studies showed that Schiff bases derived from salicylaldehyde and complexes with some transition metals displayed significant biological properties; thus, making them attracting attention in pharmaceutical and medicinal fields. Some of the reported significant biological properties are antibacterial, antifungal, antimalarial, anthelmintic, anti-inflammatory, analgesic, anticonvulsant, antioxidants, anticancer, antiviral, anti-parasitic and antitumor activities (Ahmad et al., 2020; El-Sonbati et al., 2019; Hossain et al., 2019; Ibrahim & Saad, 2023; Iglesias et al., 2019; Izuagba et al., 2021; Kubra et al., 2018; Latif et al., 2019; Nazirkar, Mandewale, & Yamgar, 2019; Omidi & Kakanejadifard, 2020; Ommenya et al., 2020; Ortiz et al., 2023; Saranya et al., 2020; Sayed et al., 2020; Shajari & Yahyaei, 2020; Suleiman et al., 2023; Thangadurai et al., 2020; Uddin et al., 2018; Venkittapuram et al., 2020).

Nowadays, with the improvement of computational methods, it is probable to reliably model and determine the molecular properties of different compounds, which help augment experimental observations. Therefore, in order to correlate the theoretical and experimental results, the molecular structures of the compounds were modelled and theoretical calculations using DFT were carried out on the optimized structures. These were employed for the electronic, IR and NMR spectra. A comparison of the resemblances between the theoretical and experimental spectra of the compound could further be used for structural identification. Therefore, this study investigated the quantum chemical studies of (E)-1-((phenylimino)methyl)naphthalen-2-ol and (E)-1-(((4-chlorophenyl)imino)methyl)naphthalen-2-ol.

Material and Methods

Reagents and Instruments

2-hydroxyl-1-naphthaldehyde, aniline, 4-chloroaniline, and methanoic acid were purchased from Merck and used as supplied. The solvents DMSO (dimethylsulfoxide) and absolute ethanol were of analytical grade and were used without further purification. The infrared spectrum was recorded on a Perkin-Elmer 400 FT-IR/FT-FIR, and the NMR spectrum was obtained using a Bruker Avance 111 600 in solution with deuterated DMSO using tetramethylsilane (TMS) as internal standard at 600 MHz. The elemental analysis was carried out with a Finnigan Flash EA 1112 series. Additionally, the electronic spectrum was recorded on a Shimadzu UV-2600 series in DMSO.

Synthesis of the Compound

5.0 mmol of the corresponding amine in 10 mL of ethanol was added in drops to 5.0 mmol of the 2-hydroxy-1-naphthaldehyde in 20 mL of the same solvent. The resulting solution was stirred for 2 hours after the addition of three drops of methanoic acid. The coloured solids precipitated were separated by filtration and recrystallized from hot ethanol.

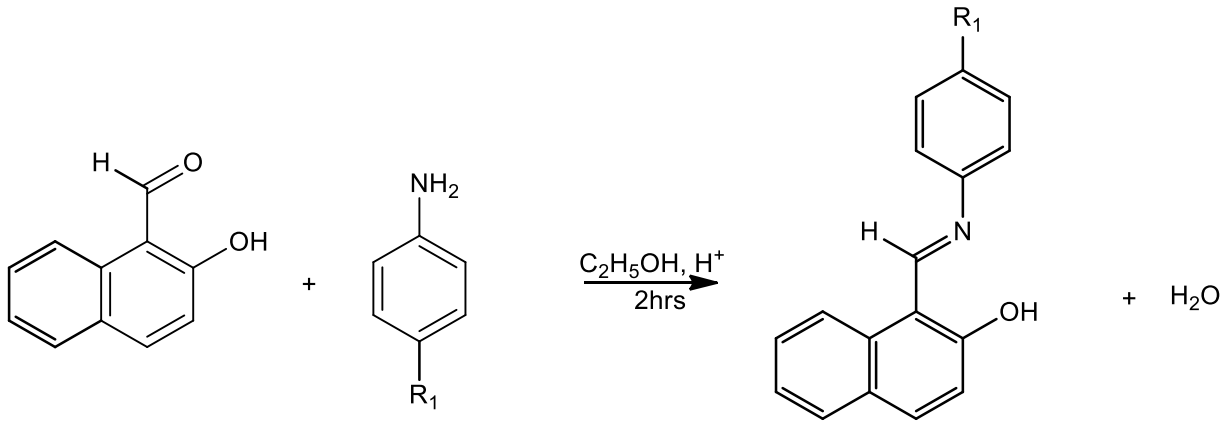

$L_1 = R_1 = H$; $L_2 = R_1 = Cl$

Scheme 1: *Synthetic route of the compounds*

Details of Computational Method

The compound was modelled and optimized using Gaussian 09 and Spartan'14 computational software packages. Density Functional Theory was employed for the geometry optimization, chemical shifts, electronic transitions and frequency calculations of the compound based on a preliminary conformational search of the molecule with a molecular mechanics force field. The DFT calculations were performed on the most stable conformer in the ground state using Becke's three-parameter hybrid functional employing the Lee-Yang-Parr correlation functional (B3LYP) and the Empirical Density Functional 1 methods (EDF1) with 6-31G** basis set (Demehin, 2021; Demehin et al., 2024; Shajari & Yahyaei, 2020).

Results and Discussions

Characterization of the Compound

(E)-1-((phenylimino)methyl)naphthalen-2-ol ($C_{17}H_{13}NO$; L_1) = Yield: 85%, colour: yellow solid, mol wt: 247.29 g/mol. Elemental analysis, % (Found) C: 82.64, H: 5.32, N: 5.67. Calculated, C: 82.57, H: 5.30, N: 5.66. FT-IR (ATR, cm^{-1}): 3550, 3151, 2318, 2159, 2040, 1961, 1620, 1546, 1489, 1408, 1347, 1336, 1318, 1214, 1143, 1101, 1088, 1079, 1043, 1027, 982, 969, 907, 866, 839, 757, 688, 664, 648, 569, 544, 528, 519, 494, 479, 467. ^{1}H NMR (DMSO-d_6, δ, ppm): 13.30 (s, 1H, OH), 9.29 (s, 1H, −HC=N), 8.07-7.06 (m, 9H, aromatic). ^{13}C NMR (DMSO-d_6, ppm): 154.32, 144.94, 139.32, 137.04, 133.34, 129.72, 129.49, 128.26, 127.26, 126.69, 124.56, 123.53, 122.69, 120.26, 118.80. UV (nm): 319 ($n-\pi^*$), 441 ($\pi-\pi^*$).

(E)-1-(((4-chlorophenyl)imino)methyl)naphthalen-2-ol ($C_{17}H_{12}NOCl$; L_2) = Yield 82%, colour: yellow solid, mol wt: 281.74 g/mol. Elemental analysis, % (Found) C: 72.52, H: 4.27, N: 5.00. Calculated, C: 72.47, H: 4.29, N: 4.97. FT-IR (ATR, cm^{-1}): 3750, 3000, 2933, 1605, 1564, 1484, 1316, 1160, 1087, 1007, 956, 855, 822, 775, 746, 726, 679, 522, 495, 477. ^1H NMR (DMSO-d_6, δ, ppm): 13.30 (s, 1H, OH), 9.31 (s, 1H, −HC=N), 8.09-7.11 (m, 8H, aromatic). ^{13}C NMR (DMSO-d_6, ppm): 155.77, 144.70, 136.44, 132.89, 132.06, 129.67, 129.45, 129.19, 128.07, 127.49, 123.70, 121.63, 121.52, 118.98, 116.59. UV (nm): 387 ($n-\pi^*$), 442 ($\pi-\pi^*$).

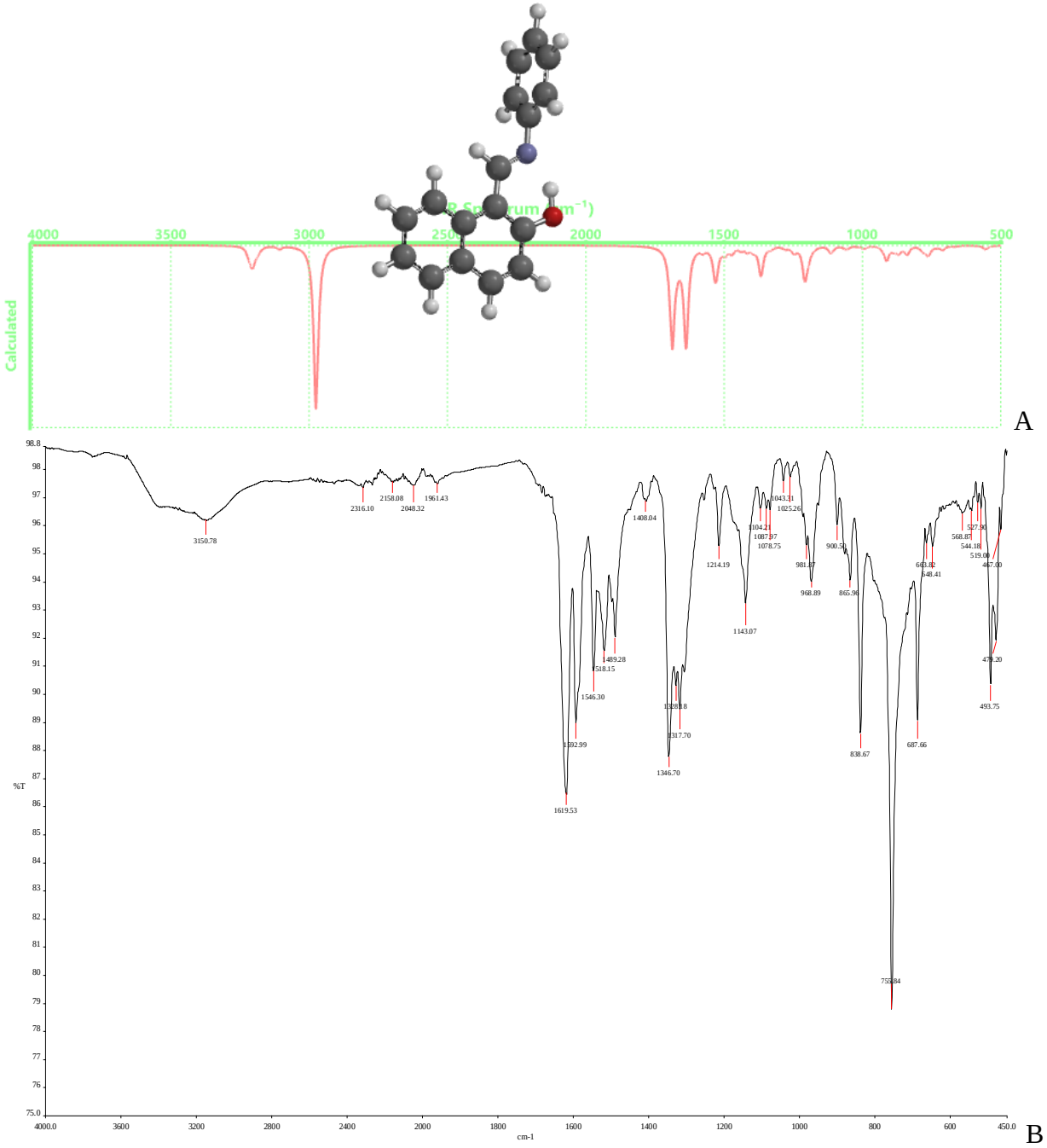

Figure 1: *IR spectra of L_1, theoretical (A) and experimental (B)*

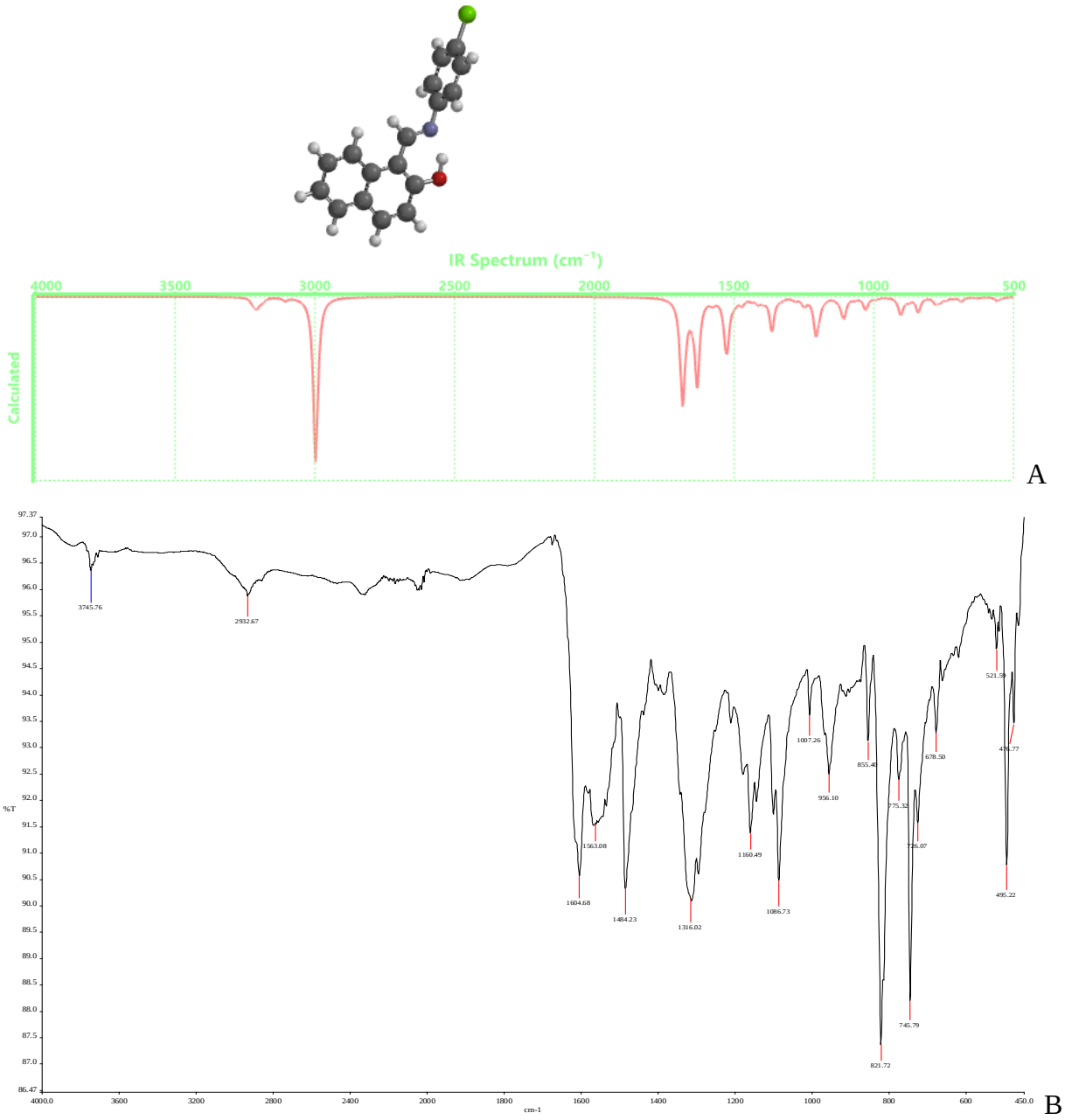

Figure 2: *IR spectra of L_2, theoretical (A) and experimental (B)*

Results and Discussions

The compounds were obtained in good yields as yellow solids. They were stable in air and soluble in most organic solvents but insoluble in water.

Spectroscopic Studies

FT-IR Spectra

The FT-IR spectra data of the compounds (Figs. 1-2) displayed the azomethine ν(−HC=N) vibrational frequencies at 1620 cm^{-1} and 1605 $cm^{-1,}$ respectively. Absorption bands at 1143 cm^{-1} and 1160 cm^{-1} in the spectra were attributed to the phenolic ν(C−O) stretching vibrations of L_1 and $L_{2,}$ respectively. (Demehin, 2021; Demehin, Oladipo, & Semire, 2020; Izuagba et al., 2021; Suleiman et al., 2023). Furthermore, the hydroxyl ν(O−H) vibrational frequencies of the compounds were shown at 3550-3151 cm^{-1} and 3746-3000 $cm^{-1,}$ respectively. However, the aromatic (C=C) absorption bands were displayed in the range 1593-1408 cm^{-1} for $L_{1,}$ while those of L_2 were exhibited at 1564-1484 cm^{-1}. Similarly, the ν(C−H) bending vibrations of the compounds appeared around 875-625 cm^{-1} (Ahmad et al., 2020; Ibrahim & Saad, 2023; Ommenya et al., 2020; Saranya et al., 2020; Thangadurai et al., 2020).

NMR Spectra

The ^{1}H NMR spectra (Figs. 3-4) of the compounds revealed a singlet signal for the phenolic –OH protons at δ 13.30 ppm. The results revealed a singlet signal at δ 9.29 ppm (L_1) and 9.31 ppm (L_2) assigned to the azomethine (−HC=N) protons. The protons of the aromatic rings appeared as multiplets at δ 8.07-7.06 ppm and 8.09-7.11 ppm, respectively (Demehin, 2021; Demehin et al., 2020; El-Sonbati et al., 2019; Nazirkar et al., 2019).

The ^{13}C NMR spectra (Fig. 5-6) of the compounds were consistent with the ^{1}H NMR. The ^{13}C NMR spectrum of the compounds exhibited peaks at 154.32 ppm (L_1) and 155.77 ppm assigned to the azomethine carbon, which further confirmed the formation of the Schiff base compounds and the aromatic carbon peaks in the range 144.94-118.80 ppm for L_1 and 144.70-116.59 ppm for L_2 (Demehin et al., 2020; Latif et al., 2019; Oloyede-Akinsulere, Babajide, & Salihu, 2018; Ommenya et al., 2020; Ortiz et al., 2023).

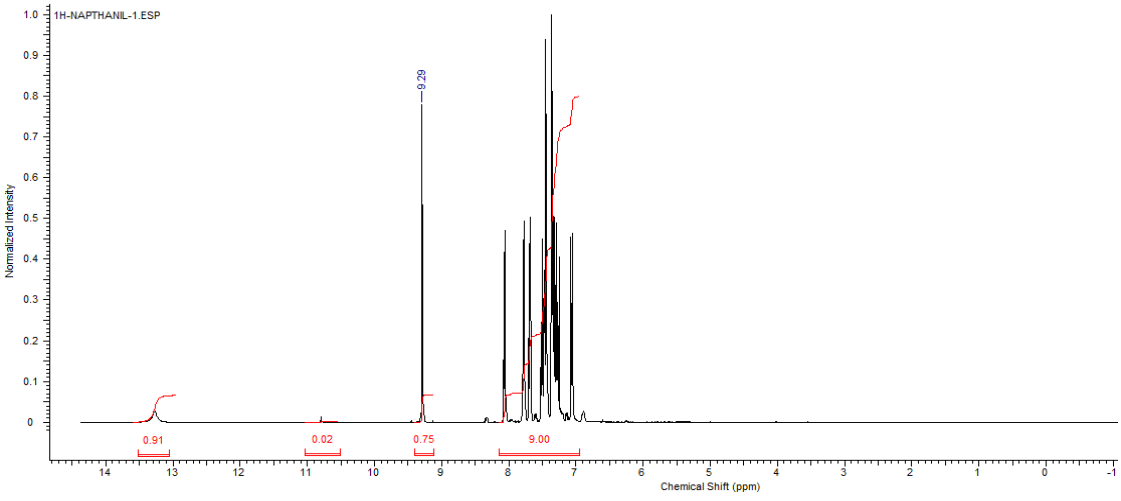

Figure 3: *^{1}H NMR spectrum of L_1*

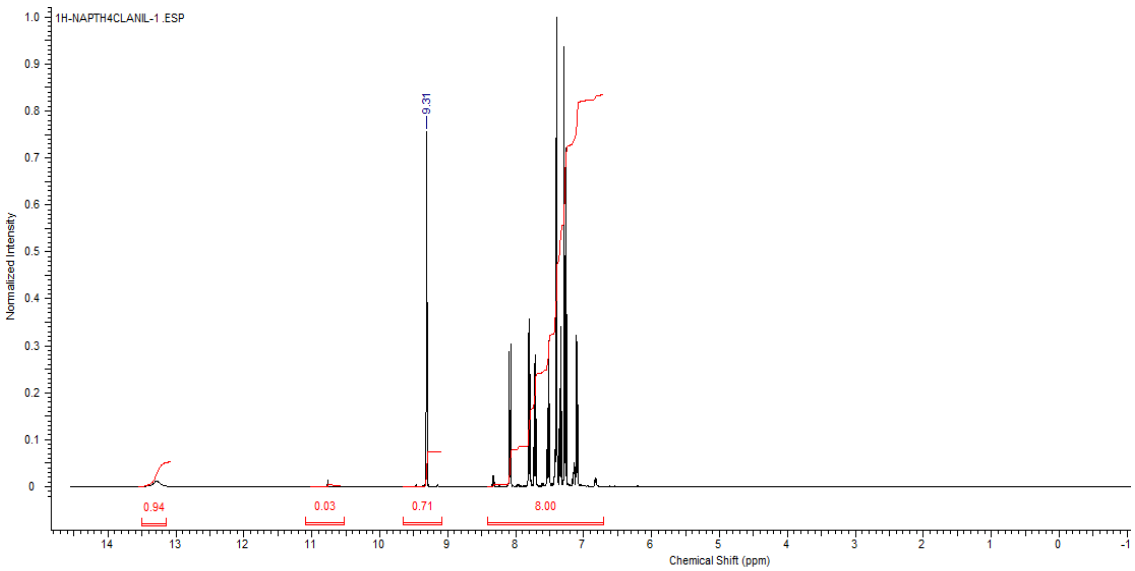

Figure 4: *^{1}H NMR spectrum of L_2*

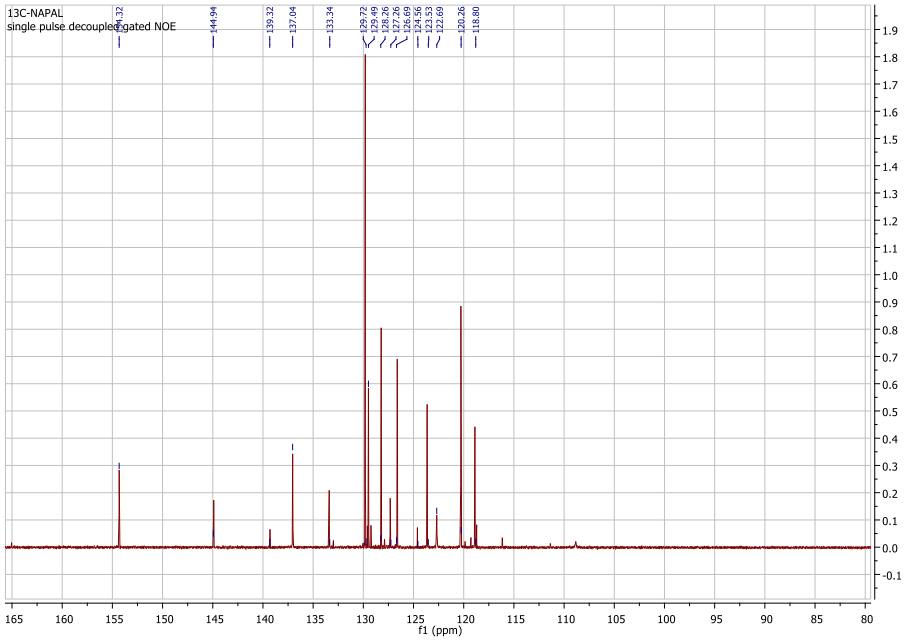

Figure 5: *^{13}C NMR spectrum of L_1*

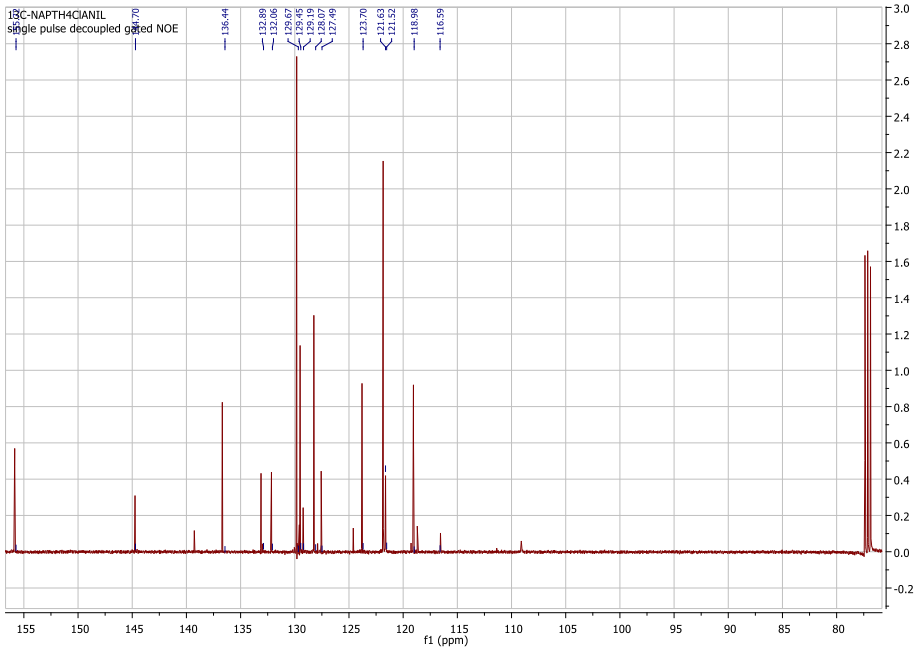

Figure 6: *^{13}C NMR spectrum of L_2*

Electronic Spectra

The electronic spectra data of the compounds showed two absorption bands around 387-319 and 458-441, which were attributed to π→π* and n→π* transitions, respectively (Demehin, Oladipo, & Semire, 2019; Demehin et al., 2020).

Computational Studies

Theoretical IR Spectra

The theoretical IR vibrational frequency values of the compounds (Table 1) were in good agreement with the experimental values (Figs. 1-2). The theoretical azomethine ν(−HC=N) absorption bands of L_1 and L_1 were observed in the range 1687-1637 cm^{-1} and 1684-1649 cm^{-1} at B3LYP/6-31G** level, while the bands were shown at 1620 cm^{-1} and 1605 $cm^{-1,}$ respectively, in the experimental spectra. The phenolic C−O stretching vibrations in the theoretical data for the compounds were displayed around 1367-1114 cm^{-1} and 1364-1114 cm^{-1}; however, these stretching vibrations were exhibited experimentally at 1143 cm^{-1} and 1160 $cm^{-1,}$ respectively. Moreover, the theoretical ν(O−H) stretching vibrations in the compounds were shown from 2975 cm^{-1} and 2997 $cm^{-1,}$ while the absorption bands were observed experimentally in the range 3550-3151 cm^{-1} and 3746-3000 $cm^{-1,}$ respectively. In the same way, the theoretical (C=C) absorption bands in the aromatic rings appeared at 1634-1417 cm^{-1} and 1632-1414 $cm^{-1,}$ respectively. However, these absorption bands were displayed around 1593-1408 cm^{-1} for L_1 and 1564-1484 cm^{-1} for L_2 in the experimental spectra. The theoretical ν(C−H) and ν(C=C) bending vibrations were indicated at 996-629 cm^{-1} for the compounds, while the bands were displayed around 875-625 cm^{-1} experimentally.

Table 1: *Theoretical IR data of the compounds*

IR bands (cm^{-1})	L_1		L_2	
	B3LYP	EDF1	B3LYP	EDF1
ν(C−H)	3219-3108	3178-3068	3225-3107	3186-3069
ν(O−H)	2975	2610	2997	2634
ν(C=N)	1687-1637	1645-1603	1684-1649	1643-1609
ν(C=C)	1634-1417	1597-1408	1632-1414	1598-1406
ν(C−O)	1367-1114	1343-1190	1364-1114	1372-1190
ν(C−H) and ν(C=C) bending	996-632	992-616	997-629	981-615

Theoretical NMR Spectra

The theoretical chemical shifts of the compounds (Table 3) are in good agreement with the experimental values. The data obtained at B3LYP/6-31G** level showed the aromatic protons in L_1: H3, H2, H1, H6, H10, H9, H5, H12, H13, H11, H4 at 9.11, 8.55, 8.38, 8.69, 8.78, 8.20, 8.00, 8.42, 8.25,8.42, 8.00 ppm respectively. These protons were experimentally observed around 8.07-7.06 ppm. The protons of the azomethine (−HC=N) and −OH groups (H7 and H19) appeared at 10.24 ppm and 15.73 ppm in t,he theoretical calculation, while the protons were experimentally observed at 9.29 ppm and 13.30 ppm respectively. However, the peaks for the aromatic carbon appeared theoretically in the range 156.10-113.94 ppm and were experimentally observed in the range 144.94-118.80 ppm. Furthermore, the azomethine carbon appeared at 159.68 ppm in the theoretical calculation, while the peak was experimentally observed at 154.32 ppm.

Additionally, the aromatic proton in L_2: H3, H2, H1, H6, H10, H9, H5, H12, H11, H4 were observed at 9.09, 8.57, 8.40, 8.70, 8.79, 8.19, 7.92, 8.27, 8.27, 7.92 ppm in the theoretical spectra, these protons appeared in the range 8.09-7.11 ppm in the experimental study. The protons of the

Table 3: *Theoretical NMR spectra data of the compounds*

Positions of H & C	L_1 δ (ppm) B3LYP	EDF1	L_2 δ (ppm) B3LYP	EDF1
H1	8.38	8.49	8.40	8.52
C1	117.74	116.15	117.99	116.67
H2	8.55	8.64	8.57	8.67
C2	122.87	120.28	123.13	120.84
H3	9.11	9.26	9.09	9.23
C3	113.94	111.59	113.83	111.95
H4	8.00	8.09	7.92	7.99
C4	129.57	126.38	129.60	126.57
H5	8.00	8.09	7.92	7.99
C5	118.28	115.09	122.81	120.71
H6	8.69	8.72	8.70	8.75
C6	125.14	122.41	125.24	122.86
H7	10.24	10.32	10.20	10.26
C7	106.48	106.25	106.39	106.26
H8	-	-	-	-
C8	159.68	157.10	159.81	157.42
H9	8.20	8.28	8.19	8.25
C9	115.19	113.96	115.07	114.04
H10	8.78	8.80	8.79	8.82
C10	129.59	128.61	131.92	129.37
H11	8.42	8.49	8.27	8.34
C11	156.10	150.64	156.49	151.37
H12	8.42	8.49	8.27	8.34
C12	148.01	144.15	146.54	142.80
H13	8.25	8.30	-	-
C13	118.83	166.76	134.60	133.08
H14	-	-	-	-
C14	115.73	113.55	116.98	115.23
H15	-	-	-	-
C15	115.73	113.55	116.98	115.23
H16	-	-	-	-
C16	123.27	120.73	123.87	121.56
H17	-	-	-	-
C17	123.27	120.73	123.87	121.56
H18	-	-	-	-
C18	-	-	-	-
H19	15.73	17.31	15.51	17.01
C19	-	-	-	-

Azomethine (−HC=N) and −OH groups (H7 and H19) appeared at 10.20 ppm and 15.51 ppm in the theoretical study, while the protons were observed at 9.31 ppm and 13.30 ppm respectively, in the experimental spectrum. Nevertheless, the peaks for the aromatic carbon appeared in the range 156.49-113.83 ppm in the theoretical spectrum, which were experimentally observed in the range 144.70-116.59 ppm. Moreover, the azomethine carbon appeared at 159.81 ppm theoretically, while the peak was observed at 155.77 ppm in the experimental spectrum.

Theoretical Electronic Spectra

The theoretical electronic spectra data of the compounds were comparable to the experimental data. The agreement between the theoretical and experimental electronic spectra data substantiated the suggested structures. The theoretical spectrum of L_1 as calculated at B3LYP/6-31G** level showed five absorption bands at 244, 266, 270, 297, 322 nm; these bands were related to the promotion of electrons from HOMO-2 → LUMO+1, HOMO → LUMO+1, HOMO-3 → LUMO, HOMO-2 → LUMO, HOMO → LUMO respectively. Similarly, L_2 displayed five absorption bands at 253, 256, 268, 299, 325 nm as calculated at B3LYP/6-31G** level, which were associated with the elevation of electrons from HOMO → LUMO-2, HOMO-3→ LUMO, HOMO → LUMO+1, HOMO-2 → LUMO, HOMO → LUMO respectively.

Frontier Molecular Orbitals

The frontier molecular orbitals are the highest occupied molecular orbital (HOMO) and the lowest unoccupied molecular orbital (LUMO). They govern the way molecules relate to other species. The HOMO is the orbital energy that contributes electrons; meanwhile, it is the orbital of highest energy containing electrons. Alternatively, the LUMO is the orbital of lowest energy. The energy gap between the HOMO and LUMO is likely to play a significant role in the intra- and inter-charge transfers by the frontier molecular orbital theory (Temel *et al*., 2015). The energy band gaps between the HOMO and LUMO are more substantial in considering electronic transitions than the individual orbital components of a molecule. Since the difference between the LUMO and HOMO reveals the reactivities and stabilities of molecules in chemical reactions, thus, the lower the energy gap, the more reactive and less stable the molecule. Consequently, Fig. 7 showed the suggested structures, optimized structures, HOMO and LUMO of the synthesized compounds. The energies of the HOMO and LUMO are -5.9 eV and -2.0 eV, respectively, while the calculated energy band gaps are 3.9 eV and 3.9 eV, respectively.

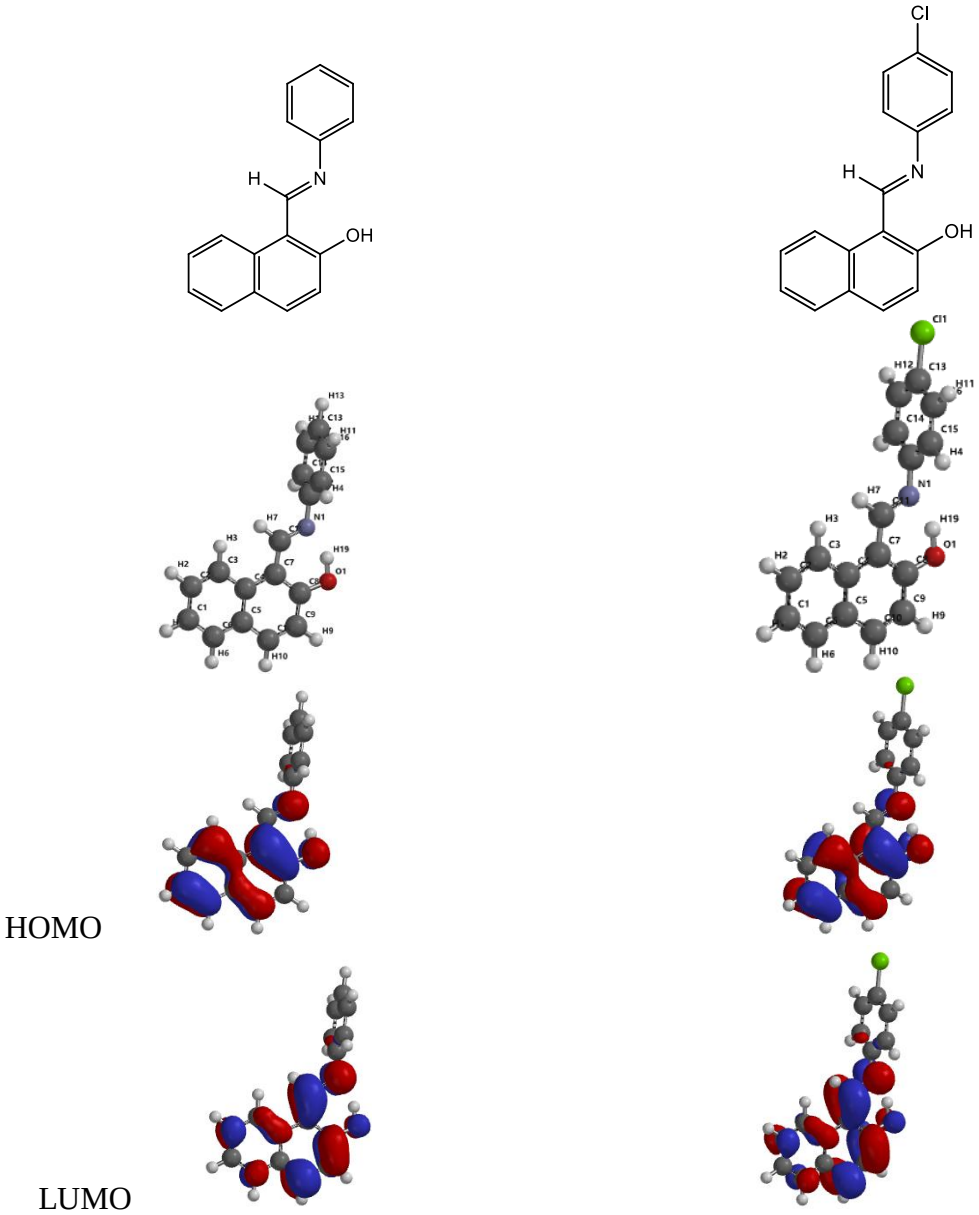

Figure 4: *Proposed structures, Optimized structures of the compounds at B3LYP/6-31G** level*

Conclusion

Two Schiff bases, (E)-1-((phenylimino)methyl)naphthalen-2-ol and (E)-1-(((4-chlorophenyl)imino) methyl)naphthalen-2-ol were synthesized and characterized by different spectroscopic techniques. The elemental analyses, IR, ^{1}H NMR, ^{13}C NMR and electronic spectra confirmed the formation of the compounds. A comparison of the experimental and theoretical results showed that the theoretical data were in very good agreement with the experimental values, hence supporting the proposed structures.

References

Abo-Aly, M. M., Salem, A. M., Sayed, M. A., & Abdel Aziz, A. A. (2015). Spectroscopic and structural studies of the Schiff base 3-methoxy-N-salicylidene-o-amino phenol complexes with some transition metal ions and their antibacterial, antifungal activitys. *Spectrochimica Acta Part A: Molecular and Biomolecular Spectroscopy, 136*, 993-1000.

Ahmad, N., Anouar, E. H., Tajuddin, A. M., Ramasamy, K., Yamin, B. M., & Bahron, H. (2020). Synthesis, characterization, quantum chemical calculations and anticancer activity of a Schiff base NNOO chelate ligand and Pd(II) complex. *PloS One, 15*(4), 1-17.

Belal, A. A. M., El-Deen, I. M., Farid, N. Y., Rosan, Z., & Refat, M. S. (2015). Synthesis, spectroscopic, coordination and biological activities of some transition metal complexes containing ONO tridentate Schiff base ligand. *Spectrochimica Acta Part A: Molecular and Biomolecular Spectroscopy, 149*, 771-789.

Bitu, M. N. A., Hossain, M. S., Zahid, A. A. S. M., Zakaria, C. M., & Kudrat-E-Zahan, M. (2019). Anti-pathogenic Activity of Cu (II) Complexes Incorporating Schiff Bases : A Short Review. *American Journal of Heterocyclic Chemistry, 5*(1), 11– 23.

Demehin, A. I. (2021). Computational Modelling and Antioxidant Activities of Substituted N-(Methoxysalicylidene) Anilines *Chemical Science International Journal, 30*(11), 18-29.

Demehin, A. I., Fehintola, E. O., Akinlami, O. O., Babajide, J. O., & Famobuwa, O. E. (2024). Synthesis, Spectroscopic Characterization and Computational Modelling of Ni(II) Complex of (E) -2- (((2-Hydroyphenyl) imino)methyl)-6-methoxyphenol. *Journal of Science, Technology, Mathematics and Education (JOSTMED), 19* (1), 57-69.

Demehin, A. I., Oladipo, M. A., & Semire, B. (2019). Synthesis, Spectroscopic, Antibacterial and Antioxidant Activities of Pd(II) Mixed-Ligand Complexes Containing Tridentate Schiff Bases. *Egyptian Journal of Chemistry, 62*, 423-426.

Demehin, A. I., Oladipo, M. A., & Semire, B. (2020). Synthesis, spectroscopic, biological activities and DFT calculations of nickel (II) mixed-ligand complexes of tridentate Schiff bases. *Eclética Química Journal, 45*(1), 18-46.

El-Sonbati, A. Z., Mahmoud, W. H., Mohamed, G. G., Diab, M. A., Morgan, S. M., & Abbas, S. Y. (2019). Synthesis, characterization of Schiff base metal complexes and their biological investigation. *Applied Organometallic Chemistry,, 33*(9), e5048.

Hossain, M. S., Banu, L. A., E-Zahan, M. K., & Haque, M. M. (2019). Synthesis, Characterization and Biological Activity Studies of Mixed Ligand Complexes with Schiff base and 2,2'-Bipyridine. *International Journal of Applied Science - Research and Review, 6*(1:2), 1-7.

Ibrahim, R. B., & Saad, S. T. (2023). Cobalt (II) and Nickel (II) complexes with Schiff base derived from 9,10- phenanthrenquinone and 2-mercaptoaniline, synthesis and characterization *Journal of Medical and Pharmaceutical Chemistry Research, 5*, 739-747.

Iglesias, L., Miranda-Soto, V., A., P.-M. D., Martínez-Ortiz, J. G., Díaz-Trujillo, G. C., & Villarreal-Gómez, l. (2019). Biological Activity of New Schiff Base Compounds Derived from Substituted 3-Aminopyrazoles, the Role of Pyrazole on Bioactivity. *Indian Journal of Pharmarceutical Sciences, 81*(2), 333-343.

Izuagba, G. O., Muluh, E. K., Amowie, P. O., & Glen, E. (2021). Antimicrobial Activity of 2-((2-Hydroxybenzylidene) Amino) Nicotinic Acid and Its Cobalt (II) Complexes Synthesized from O- Phenylenediamine and 5 Nitrosalicylaldehyde. *Caliphate Journal of Science & Technology, 2*, 139-151.

Kianfar, A. H., Farrokhpour, H., Dehghani, P., & Khavasi, H. R. (2015). Experimental and theorectical spectroscopic study and structural determination of nickel(II) tridentate Schiff base complexes. *Spectrochimica Acta Part A: Molecular and Biomolecular Spectroscopy, 150*, 220-229.

Kubra, K., Suganya, A., Saranya, J., & Lakshmi, S. S. (2018). Biological Activities of Schiff bases and their Copper(II) Complexes *World Journal of Pharmaceutical Research, 17*(8), 411.

Latif, M. A., Tofaz, T., Chaki, B. M., Islam, H. M. T., Hossain, M. S., & Kudrat-E-Zahan, M. (2019). Synthesis, Characterization, and Biological Activity of the Schiff Base and Its Ni(II), Cu(II), and Zn(II) Complexes Derived from 4-(Dimethylamino)benzaldehyde and S-Benzyldithiocarbazate. *Rusians Journal of General Chemistry, 89*, 1197-1201.

Nazirkar, B., Mandewale, M., & Yamgar, R. (2019). Synthesis, characterization and antibacterial activity of Cu (II) and Zn (II) complexes of 5-aminobenzofuran-2-carboxylate Schiff base ligands. *Journal of Taibah University for Science, 13*(1), 440-449

Oloyede-Akinsulere, A. I., Babajide, J. O., & Salihu, S. O. (2018). Synthesis, Antibacterial and Antioxidant Activities of Some Tridentate Substituted Salicylaldimines *Asian Journal of Applied Chemistry Research, 1*(4), 1-10.

Omidi, S., & Kakanejadifard, A. (2020). A review on biological activities of Schiff base, hydrazone, and oxime derivatives of curcumin. *Royal Society of Chemistry, 10*, 30186-30202.

Ommenya, F. K., Nyawade, E. A., Andala, D. M., & Kinyua, J. (2020). Synthesis, Characterization and Antibacterial Activity of Schiff Base, 4-Chloro-2-{(E)-[(4-Fluorophenyl)imino]methyl}phenol Metal (II) Complexes. *Journal of Chemistry, 2*, 1-8.

Ortiz, R. J., Shepit, M., Lierop, J. V., Krzystek, J., Telser, J., & Herbert, D. E. (2023). Characterization of the Ligand Field in Pseudo-Octahedral Ni(II) Complexes of Pince-Type Amido Ligands: Magnetism, Redox Behaviour, Electronic Absorption and High-Frequency and -Field EPR Spectroscopy. *European Journal of Inorganic Chemisrty, 25*(28), e202300446.

Saranya, J., Kirubavathy, S. J. C., S., Zarrouk, A., Kalpana, K., Lavanya, K., & Ravikiran, B. (2020). Tetradentate Schiff Base Complexes of Transition Metals for Antimicrobial Activity. *ARABIAN JOURNAL FOR SCIENCE AND ENGINEERING, 45*, 4683–4695.

Sayed, S. S., Shah, D., Ibrahim, K., Sajjad, A., Umar, A., & Atiq ur, R. (2020). Synthesis and Antioxidant Activities of Schiff Bases and Their Complexes: An Updated Review. *Biointerface Research in Applied Chemistry, 10*(6), 6936-6963.

Shajari, N., & Yahyaei, H. (2020). Spectroscopic and DFT Investigation on Some New Aryl (trichloroacetyl)carbamate Derivates. *Physical Chemistry Research, 8*(4), 705-718.

Suleiman, A. K., Sadi, A. H., Badamasi, H., & Ahmadu, M. (2023). Synthesis, Characterization and Antimicrobial Studies of Schiff Base Derived from 2-Amino Phenol and O-Anisaldehyde and Its Co (II), Cu (II) and Zn (II) Complexes *Dutse Journal of Pure and Applied Sciences, 9*(2), 301-310.

Thangadurai, A. S., Johnpeter, M. P., Manikandan, R., & Raj, A. P. (2020). Synthesis, Spectral Characterization and Biological Evaluation of Schiff Base Derived From 3-Methoxy Salicylaldehyde with Aniline and Its Transition Metals. *International Journal of Scientific and Technology Research, 9*(3), 5964-5970.

Uddin, M. N., Khandaker, S., Moniruzzaman, Amin, M. S., Shumi, W., Rahman, M. A., & Rahman, S. M. (2018). Synthesis, Characterization, Molecular modeling, Antioxidant and Microbial Properties of some Titanium(IV) complexes of Schiff Bases. *Journal of molecular structure, 1166*, 79-90.

Venkittapuram, P., Dhandapani, M., Suyambulingam, J., & Subramanian, C. (2020). Synthesis, characterization, thermal, theoretical and antimicrobial studies of Schiff base ligand and its Co(II) and Cu(II) complexes. *Journal of Serbian Chemical Society, 85*(2), 215-225.

Zhang, L. W., Liu, L. Z., Wang, F., & Dong, W. K. (2018). Unprecedented fluorescent dinuclear Co(II) and Zn(II) coordination compounds with a symmetric bis(salamo)-like tetraoxime. *Molecules, 23*(5), 1141.